Porous Structure and Thermal Stability of Photosensitive Silica/Polyimide Composites Prepared by Sol-Gel Process

Shu-Hui Huang, Trong-Ming Don, Wei-Chi Lai, Ching-Chung Chen, Liao-Ping Cheng

Department of Chemical and Materials Engineering, Tamkang University, Taipei, Taiwan 25137, Republic of China

Received 16 September 2008; accepted 25 April 2009
DOI 10.1002/app.30790
Published online 30 June 2009 in Wiley InterScience (www.interscience.wiley.com).

ABSTRACT: The sol-gel method was employed to synthesize an inorganic–organic photosensitive composite material, silica/polyimide. Silica was covalently bonded to polyimide by introduction of 1,4-aminophenol as a coupling agent. A photosensitive cross-linking agent, 2-(dimethylamino) ethyl methacrylate, was used to engender UV sensitivity to the composite. Using field emission scanning electron microscope imaging at very high magnifications, the composite film was found to exhibit a porous cross-sectional structure. The pores were interconnected to form numerous continuous channels within the matrix and silica particles were attached to the pore wall of the polyimide host. Depending on the preparation conditions, the size of the silica particles could vary from 20 nm to a few μm. The thermal degradation temperatures, dynamic mechanical properties, glass transition temperatures, thermal expansion coefficients, and dielectric constants of various silica/polyimide composites were measured, and the results indicated that incorporation of silica could improve the thermal and dimensional stabilities of the polyimide. Also, because the silica/polyimide composite had a porous interior structure, it had a rather low dielectric constant with the lowest achievable value being 1.82. © 2009 Wiley Periodicals, Inc. J Appl Polym Sci 114: 2019–2029, 2009

Key words: composites; dielectric properties; silicas; polyimides; morphology

INTRODUCTION

Photosensitive polymeric materials have been widely used in the printed circuit-board and optical-electronic industries as a key component in applications such as packaging, plastic hard coatings, etc. In a traditional microelectronics application, polyimide is often used as the photoresist to provide the photolithographic pattern because of their outstanding characteristics, such as high tensile strength and modulus, high glass transition temperature, low dielectric constant, and superior chemical resistance. Nevertheless, their relatively high humidity absorption (up to 3–4%) and high thermal expansion coefficient still impede their broad applications.[1–3]

Recently, preparation of inorganic/organic hybrids has been intensively studied in terms of combining the sol-gel reaction of organic-metallic compounds with polymerization reactions.[4–9] A wide range of inorganic/organic hybrids could be prepared by appropriate selection of raw materials and preparative approaches to achieve various properties and to meet the requirements of different applications. Employing the sol-gel method, hybrids containing poly(tetramethylene oxide), poly(ether ketone), poly(ether sulfone), poly(oxyethylene), poly(dimethylsiloxane), polysiloxane elastomers, and polyurea[10–14] have been prepared and reported. Possessing versatile properties (especially dielectric and mechanic-thermal properties) and being used in a wide range of applications, polyimide has been extensively investigated as matrices for hybrids in the search of novel materials for microelectronics and engineering. On the other hand, silica has been considered an ideal reinforcing component in hybrids for improving the thermal and mechanical properties of materials.[15] Various types of organic silane have been employed as coupling agents in the preparation of polyimide/silica hybrids in the last decade in which the organic part is supposed to interact with the polymer chain and the alkoxy units on the other hand with the silica network.

Recently, low dielectric constant is one the most desirable properties for next-generation electronic devices.[16,17] The incorporation of free space in the form of micropores or voids, especially pores with interconnection, is an attractive method for decreasing the dielectric constant of films. Nanoporous polymers are prepared in various ways, such as by inclusion of glass or carbon microspheres,[18] using blowing agents,[19,20] and by decomposing the thermally labile domain in a phase separated block or graft copolymer. Increasing the porosity decreases the dielectric constant, but it tends to reduce the material's mechanical strength. Therefore, it is necessary to control the amount of large pores, which would otherwise become void defects in the material.[21]

Correspondence to: L.-P. Cheng (lpcheng@mail.tku.edu.tw).

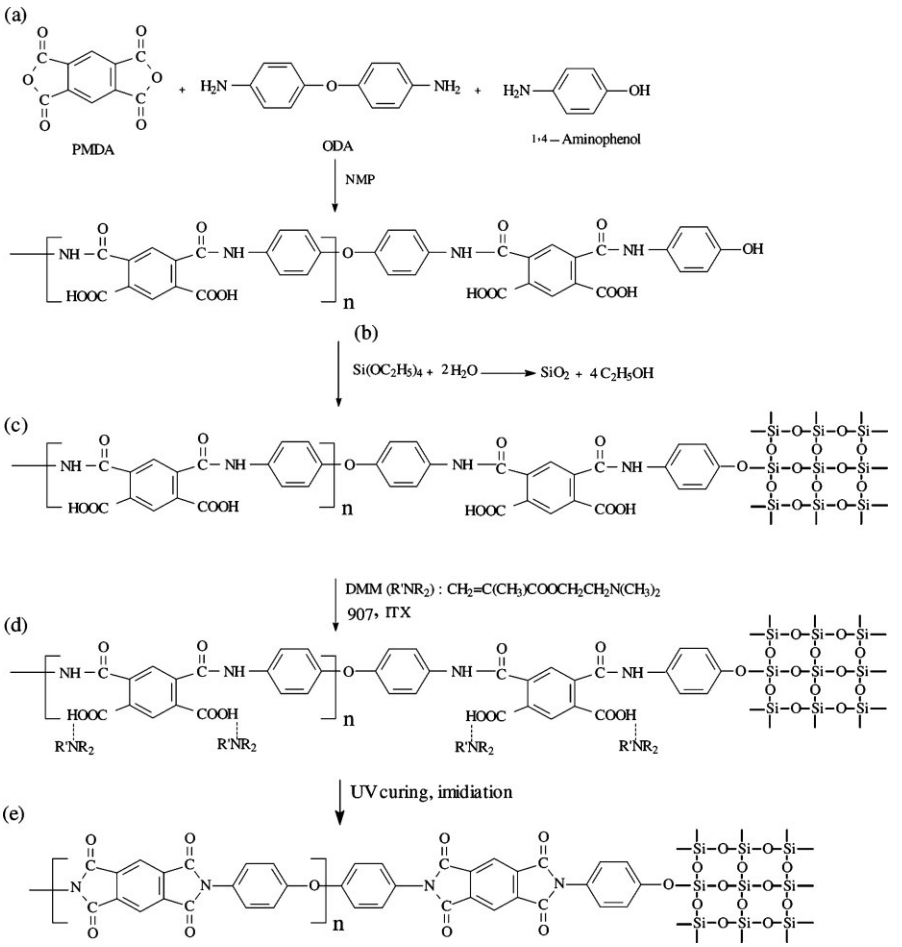

Scheme 1 Synthesis of photosensitive silica–polyimide composite by sol-gel process.

In this study, silica/polyimide composite films were synthesized using an *in situ* sol-gel reaction followed by roller coating and multistep curing, as illustrated in Scheme 1. The particle size of the polyimide/silica hybrid could be controlled by using a coupling agent, 1,4-aminophenol. 2-(Dimethylamino)ethy methacrylate (DMM) was employed as a crosslinking agent, which can form ionic bonds with the polyimide precursor. Because DMM contains C=C bonds, the system is photosensitive and can be cured by UV irradiation. Furthermore, during imidization at elevated temperatures, poly(DMM) decomposes and generates continuous pores in the formed polyimide film. The molecular structure, morphology, thermal properties, and dielectric constants of the prepared composites were studied. The effects of silica content on the morphologies and physical properties of the obtained composites were discussed.

EXPERIMENTAL

Materials

1,2,4,5-Benzenetetracarboxylic anhydride (pyromellitic dianhydride, PMDA, 97%) and 4,4′-Diaminodiphenyl ether (ODA, 99%) were obtained from Chriskev Co. (Leawood, KS) Tetraethyl orthosilicate (TEOS, 98%), 1,4-aminophenol (*p*-AP, 99%), 2-(dimethylamino)ethyl methacrylate (DMM, 99%), and *N*-methyl-2-pyrrolidone (NMP, 99%) were purchased from Acros (Geel, Belgium). 2-Methyl-1-[4-(methylthio)phenyl]-2-(4-morpholinyl)-1-propanone (Irgacure 907) and isopropylthioxanthone (ITX) used as photoinitiators were supplied, respectively, by Ciba-Geigy and Lambson Limited (Tarrytown, NY). All chemicals were used as received without further purification.

Formation of silica/polyimide composite material

Preparation of polyamic acid precursor and silica sol

ODA was dissolved in NMP under nitrogen environment in an ice bath. To this solution, 1,2,4,5-benzenetetracarboxylic anhydride (PMDA) was slowly added to carry out the polymerization reaction. After the mixture was stirred for 4 h, 1,4-aminophenol was added under continuous agitation for another 2 h [cf. reaction (a) in Scheme 1] to form the polyamic acid (PAA) precursor, which was a slightly yellowish viscous solution. This solution was stored

TABLE I
Preparation Conditions for Polyimide and Silica–Polyimide Composites

Code	PMDA : ODA : *p*-AP : DMM (Mole Ratio)	TEOS (mol)	SiO_2 Content[a] (wt %)	Remark
PI0D0S-0	1 : 1 : 0 : 0	0	0	T
PI0D1S-0	1 : 1 : 0 : 1	0	0	T
PI0D2S-0	1 : 1 : 0 : 2	0	0	T
PI0D4S-0	1 : 1 : 0 : 4	0	0	T
PI5D0S-0	1 : 0.95 : 0.05 : 0	0	0	T
PI2D2S-0	1 : 0.98 : 0.02 : 2	0	0	T
PI5D2S-0	1 : 0.95 : 0.05 : 2	0	0	T
PI5D2S-5	1 : 0.95 : 0.05 : 2	0.36	5.4	T
PI5D2S-10	1 : 0.95 : 0.05 : 2	0.77	10.9	T
PI5D2S-20	1 : 0.95 : 0.05 : 2	1.72	21.4	O
PI5D2S-30	1 : 0.95 : 0.05 : 2	2.96	31.9	O

T, transparent; O, opaque.
[a] The silica contents are calculated based on chemical equilibrium.

in an ice bath. Table I summarizes the composition of each component for various synthesis cases. During the course of the above reaction, silica sol was prepared by hydrolysis and condensation of TEOS. Nitric acid aqueous solution (pH 1.1) was added to TEOS (molar ratio: TEOS/water = 1/2) under vigorous agitation at room temperature. After a short period of haziness, a homogeneous solution was obtained. The reaction was allowed to proceed for 2 h at room temperature ([cf. reaction (b) in Scheme 1] to form a transparent silica sol.

UV curing and imidization

The synthesized PAA precursor and silica sol were reacted for 6 h [cf. reaction (c) in Scheme 1] to obtain silica-PAA composite. The molar ratios of TEOS with respect to other ingredients are shown in Table I. The silica contents were calculated based on the following chemical equilibrium equations:

$$\text{PMDA} + 0.95\ \text{ODA} + 0.05\ \text{p–AP} \rightarrow \text{PI} + 1.95\ H_2O$$

$$\text{TEOS} + 2\ H_2O \rightarrow SiO_2 + 4\ C_2H_5OH$$

Then, 2-(dimethylamino)ethyl methacrylate (DMM) and photoinitiators (Iragcure 907 and ITX) were added [cf. reaction (d) in Scheme 1] into the solution. The molar ratio of PMDA/DMM was 1/2 and the amounts of Iragcure 907 and ITX were, respectively, 1% and 5% (w/w) of the total solid content. After mixing for 0.5 h, the photosensitive mixture was spin-coated on an aluminum sheet or a glass plate.

Subsequently, it was placed in a thermostat maintained at 80°C for 30 min to remove reaction byproducts, such as water and ethanol, and solvent, NMP. The predried film was irradiated at 500 mJ/cm^2 during which free radical polymerization occurred on DMM (a pattern could be obtained, if a photomask had been used during UV exposure, for which the exposed area is cross-linked and insoluble whereas the nonexposed areas can be removed by dissolution in solvents). The UV source was supplied by the Group Up Industrial Co., Ltd (Model GUI-120, Taiwan). The range of wavelength for the mercury lamp was from 235 nm to 400 nm (broadband), and the absorption local maxima were located at 257 nm, 313 nm, and 365 nm. Finally, the obtained transparent film was heated stepwise from 25 to 260°C (i.e., hard baking) to convert the PAA to polyimide [cf. reaction (e) in Scheme 1].

Chemical structure analysis

FTIR was used to investigate the chemical structure change at various stages during formation of the silica–polyimide composite. All measurement was recorded between 4000 and 400 cm^{-1} on a Nicolet Avatar 320 FTIR Spectrophotometer (Madison, WI). For each measurement, 32 scans were collected with

TABLE II
Thermal Decomposition Temperatures and Char Yields of Polyimide and Silica–Polyimide Composites

	T_{d1}[a] (°C)	T_{d2}[b] (°C)	Char Yield (wt %)	Calculated Char Yield[c] (wt %)
Poly(DMM)	159.1	–	0	–
PI5D2S-0	310.0	538.3	43.0	–
PI5D2S-5	364.8	574.7	47.9	46.1
PI5D2S-10	384.9	589.1	52.7	49.2
PI5D2S-20	370.3	592.5	64.7	55.2
PI5D2S-30	299.6	600.2	70.1	61.2

[a] T_{d1}: 5% weight loss.
[b] T_{d2}: 15% weight loss.
[c] Assuming PI produces 43% char for all composite samples.

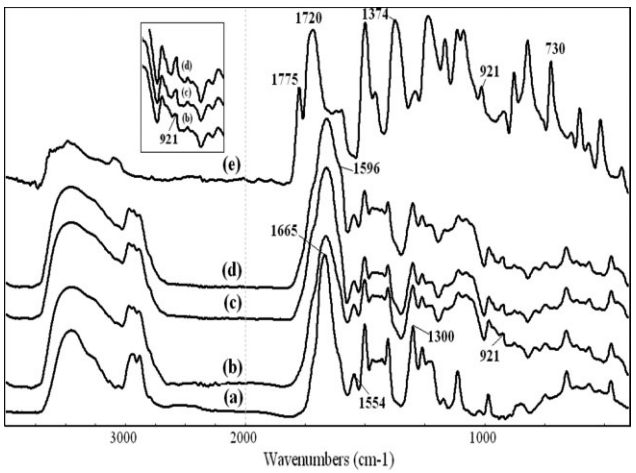

Figure 1 FTIR spectra of prepared silica–polyimide film.

a resolution of 4 cm^{-1}. Samples were prepared using the conventional KBr method.

Morphology of the silica–polyimide composite

The nanoscale fine structure of the composite was observed using a field emission scanning electron microscope (Carl Zeiss, Oberkochen, Germany, FESEM, Leo 1530) at high magnifications. The sample was vacuum-dried and then fractured in liquid nitrogen to obtain the cross section. It was attached to a sample holder using conduction copper tapes. To edge of the sample, silver paste was applied to enhance the electronic conductivity. Subsequently, a thin layer (ca. 1.0 nm) of Pt–Pd alloy was coated using a sputter coater equipped with a Quartz Crystal Microbalance thickness controller. Morphology of the fractured cross-sectional area was observed under an acceleration voltage of 8–10 kV with an inlens detector.

Thermal properties

The thermal analysis of the prepared hybrid materials, thermal decomposition temperature, glass transition temperature, and thermal expansion coefficient of the composite were studied using Thermal Gravimetric Analyzer (Hi-Res TGA 2950, TA Instrument, New Castle, DE), Dynamic Mechanical Analyzer (DMA Q800, TA Instrument), and Thermomechanical Analyzer (TMA2940, TA Instrument), respectively. The heating rate for TGA measurements was 10°C/min in the range of 25–900°C. For DMA experiments, the silica–polyimide films (20 mm × 6 mm × 0.02 mm) formed after UV-curing and imidization were secured on a film tension clamp. Measurements were performed in tensile mode at a heating rate of 5°C/min over the range, 25–450°C, with a scanning frequency of 10^5 Hz. The heating rate for TMA measurements was 5°C/min in the range of 25–450°C. All experiments were carried out under nitrogen flow.

Dielectric analysis

Dielectric relaxation data were obtained using a TA Instrument DEA-2970, which incorporates a parallel plate cell arrangement and a computer-controlled furnace to ensure good electrical contact between electrodes and sample. The experiment was conducted under a nitrogen flow rate of 90 mL/min. The thickness of the sample was controlled to be between 0.125 and 0.75 mm. The dielectric constant was determined from 0 to 150°C with a heating rate of 2°C/min and scan frequencies from 1 to 10^5 Hz.

RESULTS AND DISCUSSION

Reaction and chemical structure

Figure 1 shows the FTIR spectra of various intermediate products, as shown in Scheme l, for the synthesis of a typical silica–polyimide composite (PI5D2S-10). Spectrum (a) refers to the PAA that was formed by reaction between PMDA and ODA in the presence of 4-aminophenol, i.e., reaction (a). The absorption bands at 1665 and 1544 cm^{-1} were due to the —C=O stretching and —NH bending vibrations of amide in PAA. The band at 1300 cm^{-1} corresponded to the characteristic absorption of C—N in amide groups. These peaks were not observed in pure reactants. Reaction (b) in Scheme 1 depicts the preparation of silica sol by hydrolysis and condensation of TEOS in acidic solutions, for which the FTIR spectra have been well-documentated in the

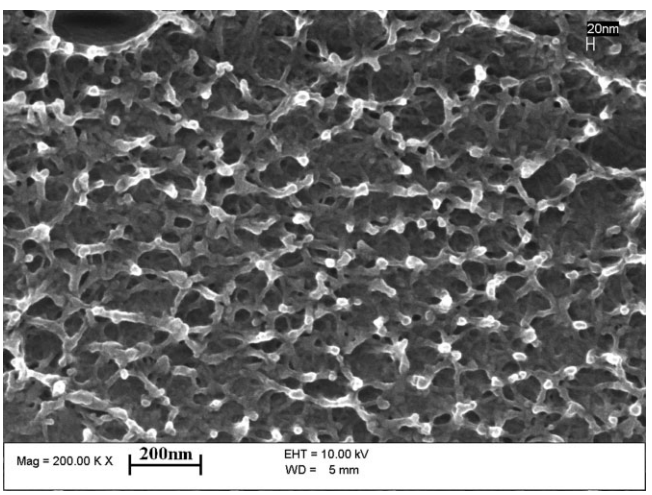

Figure 2 SEM micrograph of the cross section of a polyimide film (PI5D2S-0).

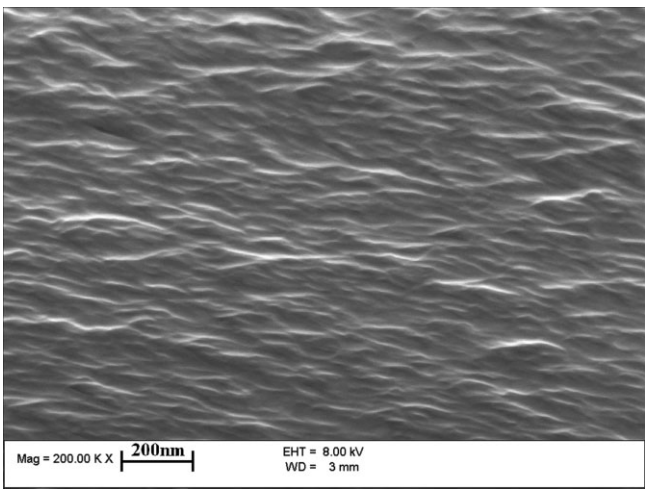

Figure 3 SEM photomicrograph of the cross section of a polyimide film prepared without using DMM (PI5D0S-0).

literature.[22] This silica sol was then added into the PAA solution to invoke condensation reaction between silica and modified PAA, i.e., reaction (c) in Scheme 1. Figure 1(b,c) shows the PAA-silica formed after 2 h and 6 h of reaction, respectively. The characteristic band at 921 cm^{-1} stands for the stretching of —Si—O—Ar. Its intensity increased as the reaction proceeded, as is clear from the inset of Figure 1. This confirms that silica has been covalently attached to the PAA matrix through the linkage of 1,4-aminophenol. Reaction (d) in Scheme 1 depicts the formation of ionic bonding between amine of DMM and carboxylic acid of PAA. The spectrum of this reaction is shown in Figure 1(d). After addition of DMM to PAA-silica, the originally free carboxylic acid group at 1600 cm^{-1}shifts to 1596 cm^{-1} due to the formation of ionic complex with DMM. Finally, imidization of PAA was carried out at 260°C, following a series of heating steps to produce silica–polyimide composite, i.e., reaction (e) in Scheme 1. The FTIR spectrum is shown in Figure 1(e). The bands at 1720 and 1775 cm^{-1} are assigned to symmetric and asymmetric stretching vibrations of —C=O in imide group, respectively.[23–27] The band at 1375 cm^{-1} denotes the stretching vibration of —C—N bond of imide and that at 724 cm^{-1} is due to the bending vibration of cyclic —C=O group.[27] All these indicate that PAA has been converted to polyimide in the heating process. However, a small Ar—COOH bond at 1680–1700 cm^{-1} can still be observed, which suggests that the imidization has not yet completed for reaction carried out at 260°C. Also, the absorption band of Si—O—Ar at 921 cm^{-1} becomes stronger than those in spectra (b) and (c), implying that condensation between Ar—OH and Si—OH continues to occur in the imidization stage.

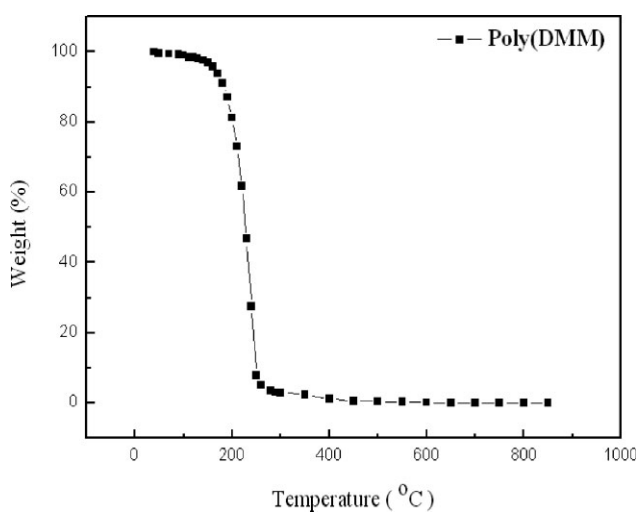

Figure 4 TGA thermogram of pure poly(DMM). Heating rate = 10°C/min.

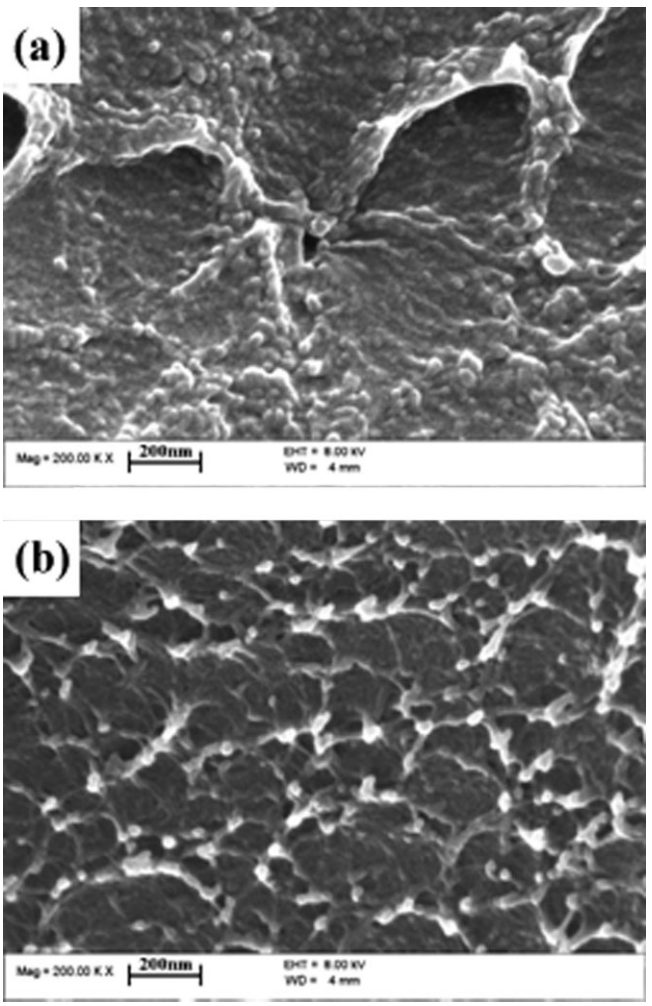

Figure 5 SEM micrograph of the cross section of (a) PI5D2S-0 film, UV cured and dried at 80°C; (b) PI5D2S-0 film, UV cured and dried at 150°C.

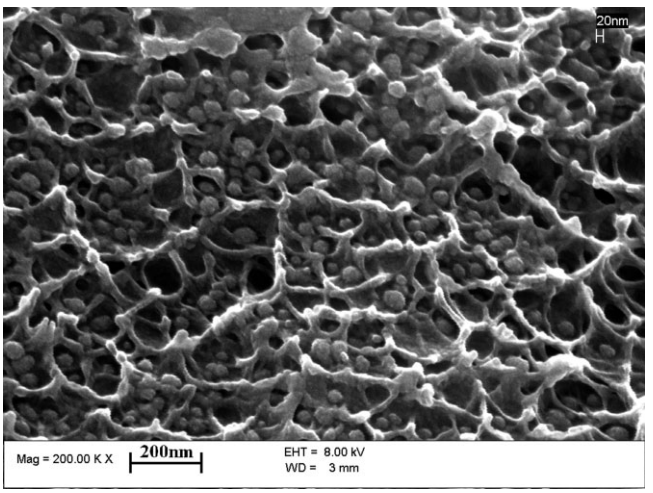

Figure 6 SEM micrograph of the cross section of a silica/polyimide composite film (PI5D2S-10).

Morphologies of polyimide and silica–polyimide composites

The nanoscale fine structures of pure polyimide and silica/polyimide composites were examined by means of high resolution FESEM. Figure 2 exhibits the cross-sectional structure of a UV-cured polyimide film, sample PI5D2S-0 in Table I, at a magnification of 200 kx. It has a porous structure consisting of interconnected pores intertwining within the framework of the polyimide matrix. Two types of pores with different sizes can be distinguished. The large pores fall largely over the range of 100–150 nm. On the pore walls, there can be observed small pores whose sizes are ca. 10–20 nm. As both types of pores are much smaller than the wavelength of visible light, the film is visually transparent. In contrast, Figure 3 shows the SEM of a polyimide film that was prepared without using DMM, sample PI5D0S-0. It appears that the cross section is dense and free of pores. The roughened texture is considered to be resulting from fracturing the sample in liquid nitrogen. Based on these morphological characteristics and referring to the reactions shown in Scheme 1, it can be deduced that the pores in Figure 2 were produced by a mechanism associated with the degradation of poly(DMM) during the hard-baking process (80–260°C). The gas produced from degradation expands at elevated temperature to generate pores in the polyimide matrix. This argument is confirmed by the TGA analysis of pure poly(DMM) synthesized from UV induced polymerization of DMM. As shown in Figure 4, degradation starts at ca. 150°C and a large-scale loss of mass takes place when the temperature reaches ca. 200°C. The thermal degradation behavior of poly(DMM) implies that a sample prepared at temperatures higher than 150°C tends to exhibit a porous structure and that the higher the reaction temperature, the higher the porosity is anticipated. Further evidence is given in Figure 5. Figure 5(a) represents the structure of the sample PI5D2S-0 that was UV cured and then purposely dried at a low temperature, 80°C, whereas Figure 5(b) is the same sample dried at 150°C. In both cases, imidization was not extensive. Apparently, sample dried at 80°C is dense and nonporous, as thermal degradation of poly(DMM) has not yet occurred. In contrast, a porous structure was obtained for the sample that was dried at 150°C, consistent with the TGA analysis. However, it should be noticed that pure poly(DMM) used as a model in TGA analysis was not exactly the same as that being ionically bonded to the PAA precursor. Also, one cannot ignore the possibility that there may still be some unreacted residual DMM monomer in the sample after the UV curing process. These monomers could vaporize to form pores as they left the film during the hard-baking process. In addition, the dense structure shown in Figure 3 for pure polyimide (without the addition of DMM) suggests that the small amount of water vapor produced by imidization at high temperatures has very little effect on the overall porous structure.

Figure 6 shows the porous structure of a silica–polyimide composite film (sample PI5D2S-10). The pore size is generally smaller than 200 nm, which is the size observed in pure polyimide in Figure 2. Spherical silica particles of 10–40 nm in diameter are also observed to reside on the pore surface. Some particles appear to interconnect to form groups of larger objects, which suggests that silica particles formed in step (b) of Scheme 1 have later reacted with each other through condensation of hydroxyl groups at particle surface (c.f. FTIR spectrum in Fig. 1). The effect of silica content on the cross-

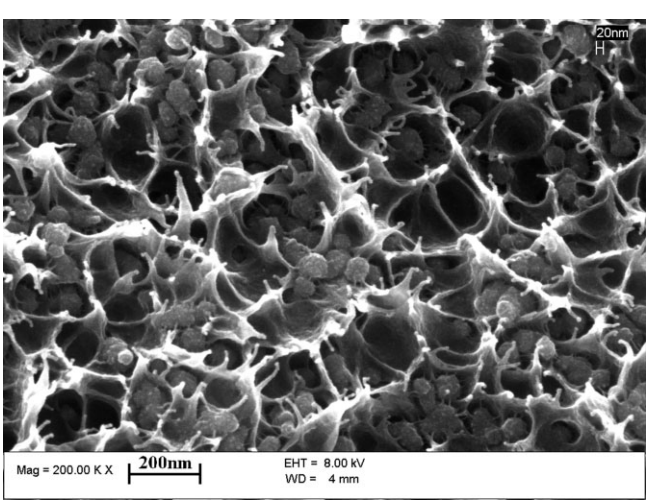

Figure 7 SEM micrograph of the cross section of a silica/polyimide composite (PI5D2S-20).

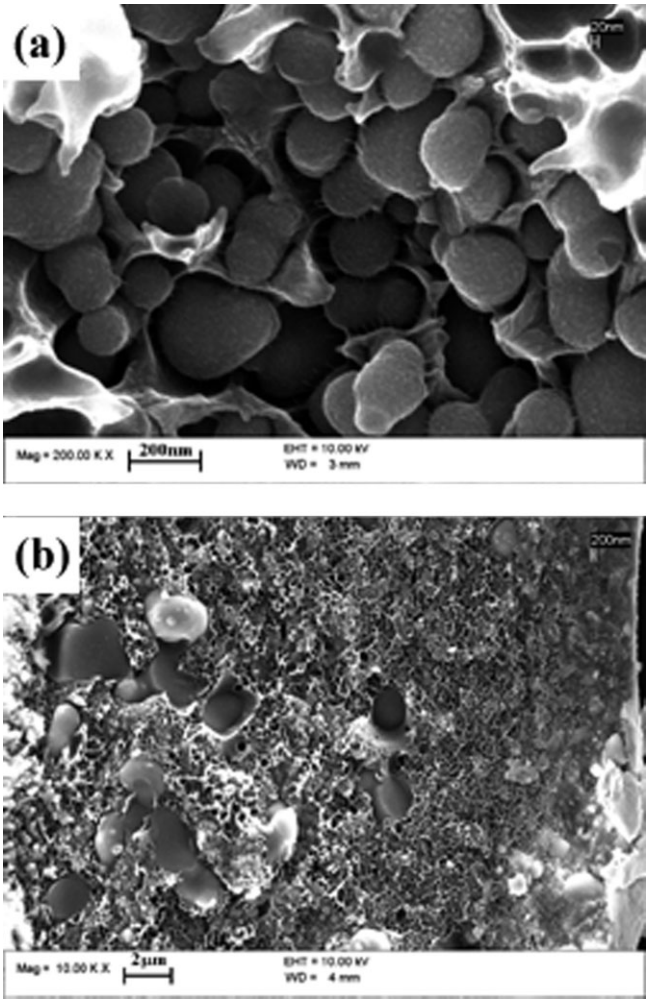

Figure 8 SEM micrograph of the cross section of a silica/polyimide composite (PI5D2S-30). (a) 200 KX and (b) 10 KX.

sectional structure of the composite was studied using SEM. Micrographs of the composite films, PI5D2S-20 and PI5D2S-30, are shown in Figures 7 and 8, respectively. It can be seen from Figure 7 that the size of the silica particles in PI5D2S-20 is ca. 1.5–2 times larger than that in PI5D2S-10 whereas the pore size remains nearly the same at ca. 100–200 nm. As PI5D2S-20 contains twice the amount of silica particles in the sol, it is expected that the small particles in the sol could develop into larger ones through condensation with neighboring particles.[9]

Figure 8(a) shows the structure of a synthesized film with a high SiO_2 content, sample PI5D2S-30. It can be seen that both the silica particles and the pores are very large (>200 nm). At a lower magnification, Figure 8(b) shows that some particles are even larger than 5 μm. Apparently, as the silica content was excessively high, the small particles in the sol could combine into very large ones through condensation of the —OH groups on the particle surface. Thermal degradation of poly(DMM) created void space surrounding the large silica particles, which made the pores appear large. On the other hand, water vapor produced due to condensation between silica particles at high temperatures might also contribute some void space atop the silica particles. It is interesting to notice that small silica nanoparticles may attach to the polymer matrix through bundles of fibrillar elements, as shown in Figure 8(a). When the composite PI5D2S-10 was further heated to 450°C, a temperature much higher than the glass transition (373°C) but lower than the thermal decomposition point of polyimide (589°C), the pores collapsed and the film exhibited a much denser structure. As shown in Figure 9, despite some weak vestiges of the contour of large pores, the film is compact and nonporous. At 450°C, the polymer is in the rubbery regime so that flexible chains can rearrange themselves from a strained to a relaxed state and the pores collapse on light pressure between glass plates.

Thermal and dimensional stabilities of composites

Thermal degradation behavior

The TGA results of synthesized polyimide and silica/polyimide composites with different silica contents are demonstrated in Figure 10 and Table II. Figure 10(a,b) depict, respectively, the weight and the rate of weight change during the course of the TGA heating process. For polyimide free of silica (PI5D2S-0), two major weight losses are observed. The first-stage decomposition occurs over the temperature range 200–450°C, accounting for ca. 10%

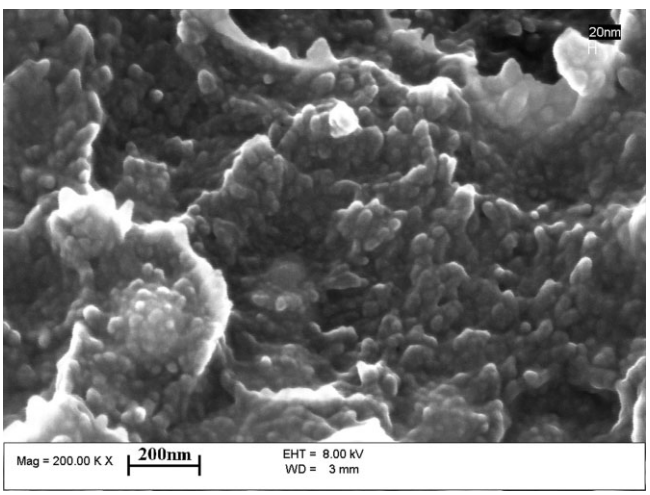

Figure 9 SEM micrograph of the cross section of a silica/polyimide composite (PI5D2S-10). Imidization was carried out up to 460°C.

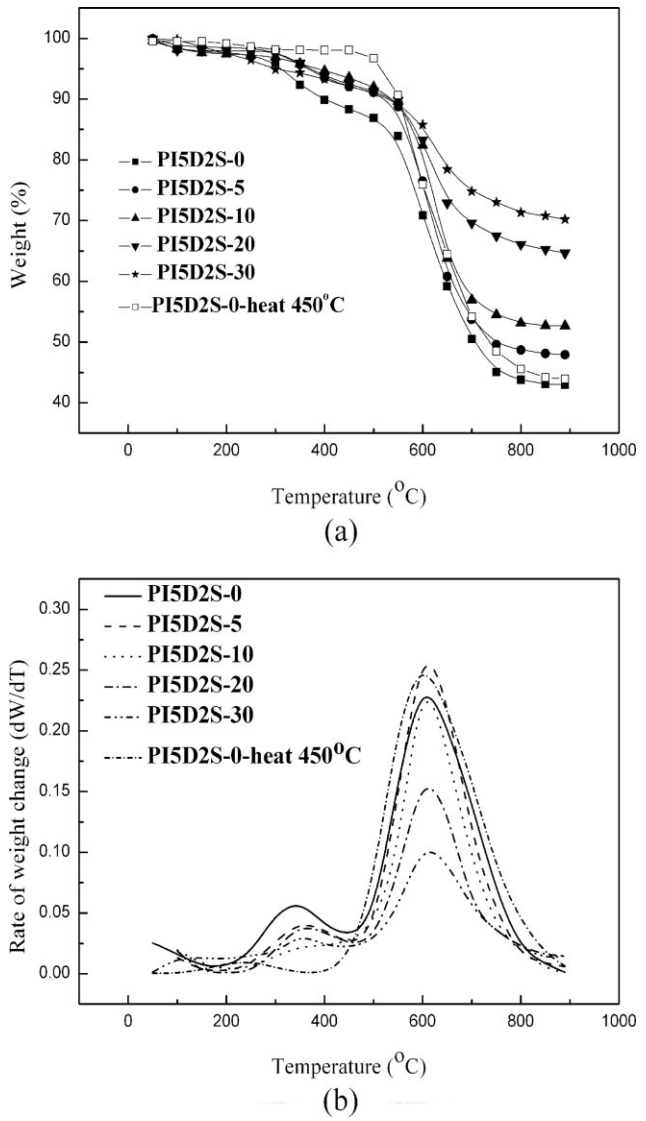

Figure 10 TGA analysis of polyimide and composites. (a) Sample weight vs. temperature and (b) rate of weight change (dW/dT) vs. temperature.

loss in weight, whereas the major decomposition, which accounts for 45% of weight loss has a maximum rate occurring at 610°C. The first stage weight loss is often attributed to the imidization of PAA. Using FTIR, Li et al. showed that in a closed system, imidization was most effective at about 300°C.[27,28] This is consistent with the TGA result of the sample PI5D2S-0 shown in Figure 10(b). The imidization reaction may continue to a temperature as high as 450°C, and above 500°C polyimide chain degrades rapidly to a final char yield of 43%. That imidization can take place beyond 350°C is further confirmed by a postbaking treatment of the sample PI5D2S-0 at 450°C for a period of 60 min. The thermal degradation curve of this sample (PI502S-0-450) is also shown in Figure 10. Apparently, there is no weight loss up to ca. 500°C, suggesting an almost complete imidization of the sample during the postbaking procedure. As SiO_2 was introduced, the thermal decomposition temperature of the formed composite increased considerably. For example, as shown in Table II, with an addition of small amount of SiO_2, the T_{d2} of the sample PI5D2S-5 is 36° higher than that of the pure polyimide PI5D2S-0. In the current study, the highest T_{d2} of all samples reaches 600°C. Obviously, the silica nanoparticles in the continuous polyimide matrix has made the material more stable against thermal decomposition through interfacial interactions and the effect is more pronounced with increasing silica content. Such phenomenon is frequently observed in nanocomposites.[25,29,30] The measured char yields of the composites, as expected, increase with increasing silica content. For example,

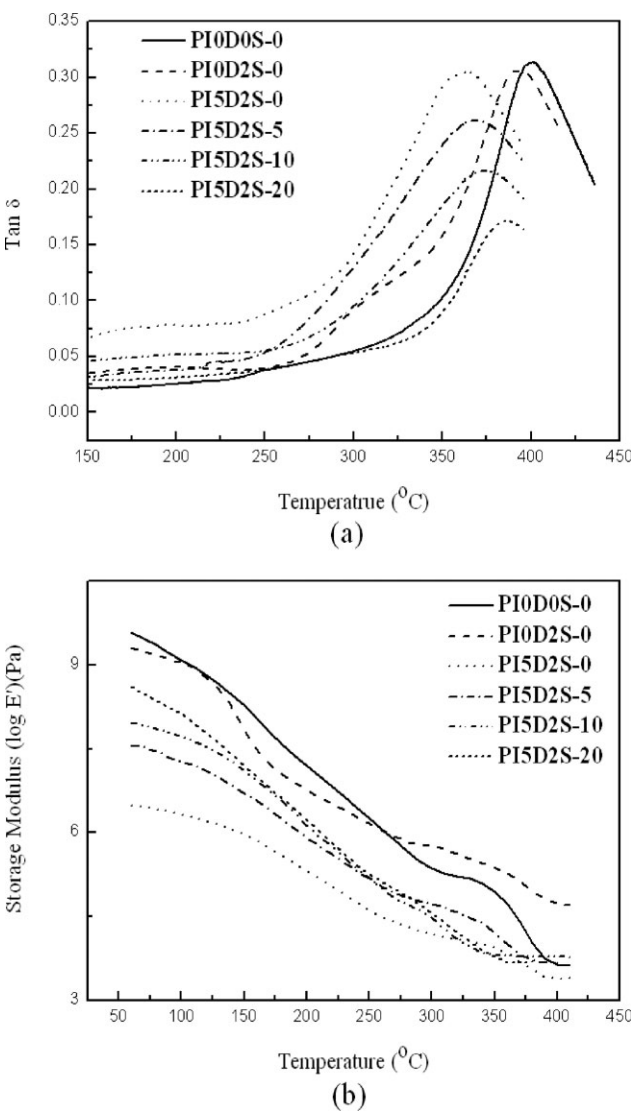

Figure 11 DMA analysis of polyimide and composites. (a) Tangent delta and (b) E'.

TABLE III
Thermal Expansion Coefficients, Glass Transition Temperatures, and Dielectric Constants of Polyimide and Silica/Polyimide Composites

Sample	α_1 (μm/m°C)	α_2 (μm/m°C)	T_g (°C) TMA	T_g (°C) DMA	Dielectric Constant DEA
PI0D0S-0	57.4	1500.5	381.9	401.2	3.43
PI0D2S-0	56.7	1443.1	383.4	393.2	2.28
PI5D2S-0	50.6	1209.1	350.1	362.4	1.82
PI5D2S-5	40.1	1111.7	354.3	368.6	2.34
PI5D2S-10	39.3	1068.2	358.5	373.9	2.52
PI5D2S-20	35.4	957.2	372.5	386.6	2.88

at 900°C, the char yield of the sample PI5D2S-30 reaches a high level of 70.1%. Assuming that PI generates 43% of char in all cases, the char yields of the composites can be calculated, as shown in Table II. The measured data are somewhat higher than the calculated ones, suggesting that PI decomposes less in the composites than its pure state. This again evidences that PI is more stable in the composites.

The dynamic mechanical behavior

The glass transition temperature (T_g) of pure polyimide and various composites were measured using DMA and the results are shown in Figure 11 and Table III. T_g of the pure polyimide (PI5D2S-0) is 362.4°C, somewhat lower than the data reported in the literature.[31] This is due to the fact that the employed coupling agent, 1,4-aminophenol, might terminate the polymerization through amidization with PMDA [cf. reaction (a) in Scheme 1]. Thus, the molecular weight of the polyimide chain in PI5D2S-0 is expected to be lower than that without using 1,4-aminophenol (PI0D2S-0).[32] As shown in Figure 11(a), the T_g of PI0D2S-0 was 393°C, ca. 30°C higher than that of PI5D2S-0. By incorporation of silica into the polymer matrix, rigidity of the composite material can be improved, especially when there are extensive interfacial interactions between organic and inorganic phases. Because the motions of polymer chains are hindered by silica, the T_g increases as well. This is illustrated in Figure 11, in which it can be seen that the T_g increases with increasing silica content in the composite. For the composite PI5D2S-20, the T_g reaches 386.6°C, which is 24°C higher than that of PI5D2S-0, but still lower than that of PI0D2S-0. In other words, the effect of silica on T_g is not as strong as that of molecular weight. This is reasonable because polyimide is itself a rather rigid polymer due to the cyclic structure along the main chain. The influence of the silica content on the storage modulus (E') is shown in Figure 11(b). The E' value increased with an increase in the silica content. This may be attributed to the interfacial bonding between polyimide molecules and silica particles through the coupling agent, 1,4-aminophenol.

Linear thermal expansion coefficient

The linear thermal expansion coefficients (α) of various composites were measured using TMA. In Figure 12, two typical results (i.e., PI5D2S-0 and

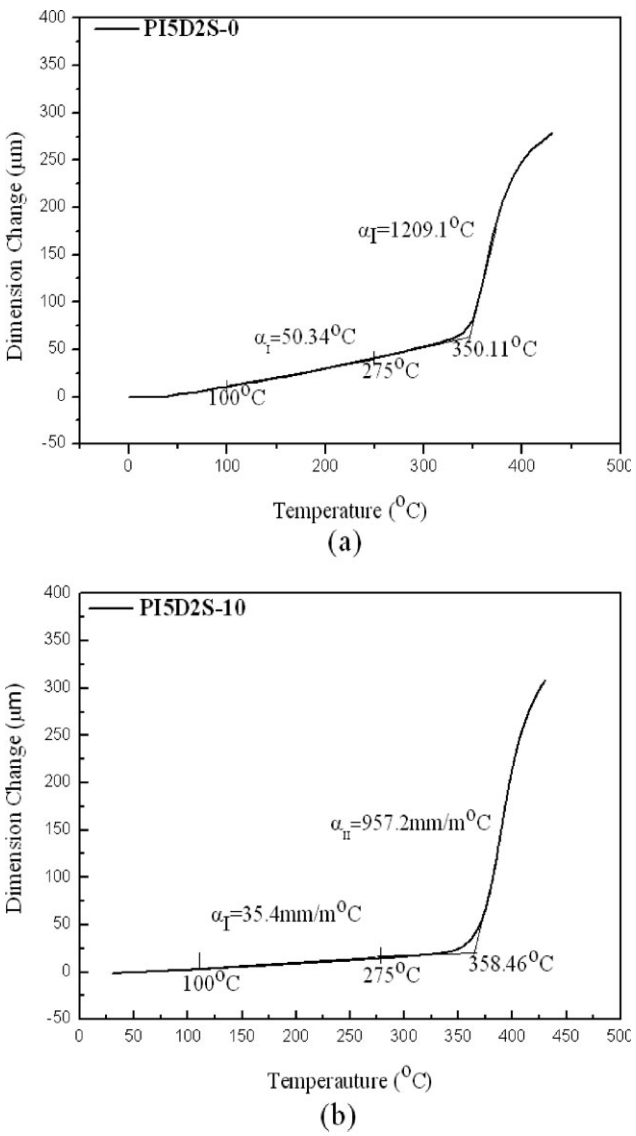

Figure 12 TMA analysis of polyimide and composites. (a) Pure polyimide (PI0D0S-0) and (b) nanocomposite PI5D2S-20.

PI5D2S-20) are presented in terms of linear dimensional change versus temperature. For pure polyimide, Figure 12(a) indicates that the thermal expansion coefficients of PI5D2S-0 are 50.6 (α_I) and 1209.1 (α_{II}) μm/m°C below and above the T_g, respectively. The T_g of this sample, as determined by the intersection of the two straight lines above and below the transition point, is 350.1°C, which is close to the data measured by DMA, cf. Table III. The thermal expansion could be reduced by the addition of silica in the composites. Figure 12(b) shows that the α_I and α_{II} of PI5D2S-20 are 35.4 and 957.2 μm/m°C, respectively, which are much smaller than the corresponding values for PI5D2S-0. Thermal expansion coefficients of several other samples are summarized in Table III. Clearly, the dimensional stability is improved for samples containing silica. In fact, factors such as the size, distribution, and quantity of the silica particles in the composite may all contribute to the thermal dimensional stability of the composites.[25,29,33]

Dielectric analysis

Among all the samples studied in this research, the sample PI5D2S-0 possesses a relatively well-distributed pore structure, as evidenced from the FE-SEM image (Fig. 2), which implies that the material may be suitable for the application in low dielectric electronic devices. The porous structure was created due to the degradation of poly(DMM) in the postbaking process as explained previously. The value of its dielectric constant (1.82) is therefore lower than that of the pure polyimide, PI0D0S-0 ($k = 3.43$), which has a dense structure (Fig. 3). The reduction in dielectric constant of the polyimide appears to be due to the continuous pores that creates loose polyimide morphology.[34,35] Table III also shows the dielectric constants of composites having different silica contents. The dielectric constant is found to increase upon increasing the silica content.

CONCLUSION

Photosensitive silica/polyimide composites with a porous interior structure were synthesized and their thermal, mechanical, and dielectric properties were studied. The pores in the samples were formed as a result of decomposition of an UV-sensitive ingredient, poly(DMM), during the postbaking process. Depending on the preparation conditions, such as initial TEOS concentration and baking temperature, the size of the pores in various composites could be varied from several tens to hundreds of nanometers, and under some circumstances, originally porous films could be made nonporous by a post heat treatment at temperatures higher than the T_g of polyimide. Depending on the added amount of TEOS, the sizes of the silica particles in the formed composite may be changed, and the finest size attainable is ca. 10 nm. By increasing the amount of silica, the thermal stability of the synthesized composite improves considerably. The highest T_g and T_d of the composites reach 386.6 and 600.2°C, respectively, which are 24 and 62°C higher than those of the pure polyimide. The thermal expansivity of the composite is much lower than that of pure polyimide, with the lowest value of all samples being 35.4 (α_I) and 957.2μm/m°C (α_{II}). By addition of poly(DMM) and a subsequent postbaking process, we manage to lower the bulk dielectric constant of the thin film from 3.43 to 1.82. Thus, these porous materials exhibit high thermal stability, good mechanical strength, and low dielectric constant making them candidates for low-*k* applications.

References

1. Chern, Y. T.; Huang, C. M. Polymer 1998, 39, 6643.
2. Eichstadt, A. E.; Ward, T. C.; Bagwell, M. D.; Farr, I. V.; Dunson, D. L.; Mcgrath, J. E. Macromolecules 2002, 35, 7561.
3. Liaw, D. J.; Liaw, B. Y.; Yu, C. W. Polymer 2001, 42, 5175.
4. Ahmad, Z.; Mark, J. E. Chem Mater 2001, 13, 3320.
5. Hsu, Y. G.; Lin, F. J. J Appl Polym Sci 2000, 75, 275.
6. Brennan, A. B.; Wilkes, G. L. Polymer 1991, 32, 733.
7. Tian, D.; Dubois, P. H.; Jerome, R. J Polym Sci Part A: Polym Chem 1997, 35, 2295.
8. Kim, H. D.; Paul, D. R. J Appl Polym Sci 1990, 40, 155.
9. Wang, L.; Tian, Y.; Ding, H.; Li, J. Eur Polym J 2006, 42, 2921.
10. Hikosaka, M. Y.; Pulcinelli, S. H.; Santilli, C. V.; Dahmouche, K.; Craievich, A. F. J Non-Cryst Solids 2006, 352, 3705.
11. Huang, H. H.; Wilkes, G. L. Macromolecules 1987, 20, 1322.
12. Hsu, Y. G.; Lin, K. H.; Chiang, I. L. Mater Sci Eng C 1997, 87, 31.
13. Mauritz, K. A.; Ju, R. Chem Mater 1994, 6, 2269.
14. Chattopadhyay, D. K.; Raju, K. V. Prog Polym Sci 2007, 32, 352.
15. Wei, Y.; Jin, D.; Yang, C.; Kel, M.; Qiu, K. Y. Mater Sci Eng C 1998, 6, 91.
16. Maier, G. Prog Polym Sci 2001, 26, 3.
17. Kuntman, A.; Kuntman, H. Microelectron J 2000, 31, 629.
18. Carleton, P. S.; Farrisey, W. J.; Rose, J. S. J Appl Polym Sci 1972, 16, 2983.
19. Hoki, T.; Matsuki, Y. Eur. Pat. 186, 308 (1986).
20. Narkis, M.; Paterman, M.; Boneh, H.; Kenig, S. Polym. Eng. Sci. 1982, 22, 417.
21. Krishnan, P. S. G.; Cheng, C. Z.; Cheng, Y. S.; Cheng, J. W. C. Macromol Mater Eng 2003, 288, 730.
22. Musto, P.; Ragosta, G.; Scarinzi, G.; Mascia, L. Polymer 2004, 45, 1697.
23. Li, H. T.; Chuang, H. R.; Wang, M. W.; Lin, M. S. Polym Int 2005, 54, 1416.
24. Wang, H.; Zhong, W.; Xu, P.; Du, Q. Macromol Mater Eng 2004, 289, 793.

25. Yena, C. T.; Chena, W. C.; Liawc, D. J.; Luc, H. Y. Polymer 2003, 44, 7079.
26. Li, W. S.; Shen, Z. X.; Zheng, J. Z.; Tang, S. H. Appl Spectrosc 1998, 52, 985.
27. Saeed, M. B.; Zhan, M. S. Eur Polym J 2006, 42, 1844.
28. Masscia, L.; Kioul, A. Polymer 1995, 36, 3649.
29. Lua, X.; Xub, J.; Wong, L. Synth Met 2006, 156, 117.
30. Shantalii, T. A.; Karpova, I. L.; Dragan, K. S.; Privalko, E. G.; Privalko, V. P. Sci Technol Adv Mater 2003, 4, 115.
31. Ergenrother, P. M.; Watson, K. A.; Smith, J. G.; Connell, J. W.; Yokota, R. Polymer 2002, 43, 5077.
32. Yanga, S. Y.; Parka, C. E.; Jungb, M. S. Polymer 2003, 44, 3243.
33. Li, Y.; Fu, S. Y; Li, Y.Q.; Pan, Q.Y.; Xu, G.; Yue, C.Y. Compos Sci Technol 2007, 67, 2408.
34. Tsai, M. H.; Whang, W. T. Polymer 2001, 42, 4197.
35. Hachisuka, H.; Ohara, T.; Ikeda, K. J. Membr Sci 1996, 116, 265.